CrossMark

CASE REPORT

Cone-beam CT to assess bony fusion following anterior cervical interbody fusion

Jan Erik Vandevenne[1,2] · Dieter Peuskens[3] · Leen Wijnen[1] · Jan Wuyts[3]

Abstract

Purpose Assessment of bony fusion following anterior cervical interbody fusion (ACIF) is usually done by plain film or CT. We present the first clinical application of Cone-Beam CT (CBCT) to evaluate bony fusion after ACIF.

Methods A 56-year-old man with disc herniation at C6-C7 underwent ACIF surgery using a compressed nanocrystalline hydroxyapatite interbody device (nanOss-C, Pioneer Surgical Marquette, MI, USA) and a nanocrystalline hydroxyapatite bone graft filler (nanOss Bioactive, Pioneer Surgical Marquette, MI, USA). Imaging follow-up was performed by CBCT (NewTom 5G, QR Srl, Verona, Italy) at 1 day, 6 weeks, 3 and 9 months postoperatively. Two independent assessors quantitatively measured the greyscale changes of the bone graft filler and qualitatively evaluated the bony fusion process.

Results Quantitative analysis of the images showed a steadily increasing matrix density of the bone graft filler over the 9 months follow-up, suggesting increasing calcification. Qualitative evaluation demonstrated different stages of the bone fusion process within the disc space around the cage, at the interface between cage and endplates, and at the interface between bone graft filler and the endplates.

Conclusions CBCT provides high-resolution cross-sectional imaging of the cervical spine after ACIF. For the first time, in vivo evaluation of the bone graft filler within the centre of the circumferentially radiodense cage and detailed cross-sectional evaluation of bone fusion was achieved. Confirmation of these promising outlooks of CBCT in a large cohort of ACIF patients is needed with regard to routine clinical application and evaluation of different interbody devices.

Keywords Cone-beam CT · ACIF procedure · Fusion · Greyscale

Introduction

Cone-Beam CT (CBCT) is a different type of CT imaging that provides a potentially low-dose cross-sectional technique for visualizing bony structures. To date, this has primarily been used in dental and maxillofacial imaging [1]. CBCT was first developed as a tool for clinical use in 1982 at the Mayo Clinic Biodynamics Research Laboratory [2]. In the intervening years, several CBCT systems have been developed for use both in the interventional suite as well as the originally intended general applications such as CT angiography [3, 4].

As CBCT imaging systems have become more widely available, there has been an increasing interest in the intraoperative and diagnostic use of CBCT for applications in the extra-cranial head and neck regions. It is likely that the strongest aspects of CBCT, i.e. the high isotropic spatial resolution reaching 100 μm or less, the relative low-radiation dose requirements and fewer metal artefacts are characteristics that have made it particularly attractive as a valuable diagnostic technique [5–7]. In the head and neck

✉ Jan Erik Vandevenne
  jan.vandevenne@zol.be

1 Faculty of Medicine, University of Hasselt, Hasselt, Belgium

2 Department of Radiology, Ziekenhuis Oost-Limburg, Campus St-Jan, Schiepse Bos 6, 3600 Genk, Belgium

3 Department of Neurosurgery, Ziekenhuis Oost-Limburg, Campus St-Jan, Schiepse Bos 6, 3600 Genk, Belgium

region, where the vascular and bony structural anatomy is particularly complex, the ability to discriminate fine anatomic detail can provide a much more effective clinical tool [8].

However, despite the advantages over other imaging modalities, there has been little use of CBCT in cervical vertebrae imaging. Furthermore, while it has been used to assess bone structure in maxillofacial and dental surgery, both pre- and post-operatively, it has not been used as a tool to assess bony fusion following cervical interbody fusion. We are therefore reporting on the first use of CBCT to evaluate osseous changes following anterior cervical interbody fusion (ACIF).

Methods/case report

Patient

The patient was a 56-year-old male who presented in our clinic with symptoms of radicular tingling in his right arm and paresthesia in his index and middle finger of his right hand. Clinical evaluation and MRI were performed to identify the involved cervical level. He was diagnosed with disc herniation on the right side at C6-C7. Initial treatment consisted of a series of 3 cervical epidural infiltrations at level C6-C7 resulting in 90 % improvement. However, troublesome paresthesia continued and he was subsequently scheduled for ACIF surgery.

Treatment

An anterior cervical interbody fusion was performed using a 7-mm compressed nanocrystalline hydroxyapatite interbody device (nanOss-C, Pioneer Surgical Marquette, MI) with a nanocrystalline hydroxyapatite bone graft filler (nanOss Bioactive, Pioneer Surgical Marquette, MI, USA). The vertebrae were fixed with a titanium anterior plate using self-drilling screws. The hospitalization occurred without complications, radicular pain disappeared and the patient was discharged 1 day post-operatively.

Cone-beam CT

The CBCT used in this report was a NewTom 5G CBCT (QR Srl, Verona, Italy). The patient was positioned with the cage in the middle of the CT bore by adjusting the height of the table and with the cage as parallel as possible with the middle of conic X-ray beam. The cone-beam volume scan was acquired with a 12 × 8 field of view and a spatial resolution of 150 μm, and reconstructed to axial images with isotropic voxel resolution of 0.5 mm. Images were reformatted in the sagittal and coronal plane with a width of 1 mm at 1-mm intervals. The mean radiation dose the patient experienced for each CBCT scan was 7.94 mGy (computed tomography dose index or CTDI). The patient was assessed 1 day after surgery and then at 6 weeks, 3 and 9 months.

Data analysis

The CBCT images were assessed quantitatively to investigate the density changes of the bone graft filler and qualitatively to evaluate signs of bony fusion. Qualitative evaluation of bony fusion included descriptive observations regarding bony changes at the interface between cage and bone, between bone graft filler and bone and within the disc space.
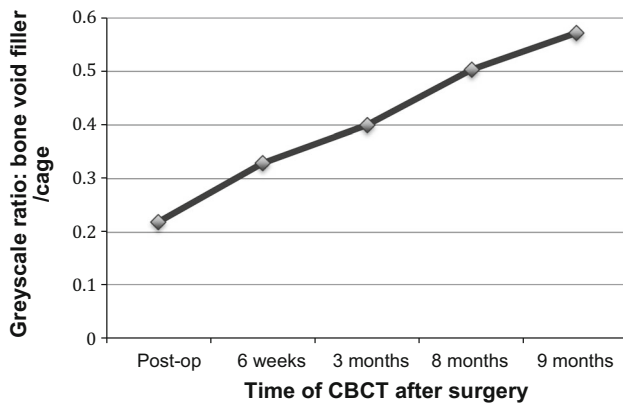
Quantitative evaluation of CBCT images was done by measuring the greyscale units, as the X-ray attenuation in CBCT is displayed by grey levels. Although these grey values do not allow for direct bone quality assessment, a recent study reported a linear relationship between CT Hounsfield Units (HU) and greyscale when using the NewTom 5G CBCT [9]. This is the same device currently used in our hospital, which is the reason we used grey value measurements as an assessment of bone density. All images were evaluated by two independent assessors at each time point. The greyscale values were measured using a region-of-interest (ROI) measuring tool and recorded. In order to normalize the greyscale data, the screws and the cage were used as reference values, as the density of these materials will not change over time. Therefore, the ratio of the greyscale value of the bone graft inside the cage and the greyscale value of the cage or screw were calculated as a means of measuring the change in the radiodensity of the hydroxyapatite bone void filler.

Results

Quantitative

There was a very high agreement between the two assessors with regard to the measured greyscale values. The Pearson correlation coefficients for the scores from the two independent evaluators ranged from 0.987 to 0.998 with an absolute difference ranging from a low of 0.02 % to a maximum of 9.8 %.

Over the 9 months of post-operative measurement, there was a steady increase in the measured values, as shown in Fig. 1. Figure 1 depicts the change in the radio-opacity for the bone void filler over the 9 months of follow-up. Specifically, this represents the greyscale values of the graft material normalized to the greyscale values of the interbody cage. Similar changes were seen when the data

Fig. 1 The increasing greyscale value of the bone void filler over the post-operative follow-up. The points on the chart depict the ratio in greyscale intensity between the hydroxyapatite bone void fill and that of the intervertebral cage

were also normalized to the greyscale level of the screws used to fix the anterior plate.

Qualitative

With regard to qualitative assessment of the images, views in the sagittal and axial planes are presented in Figs. 2, 3.
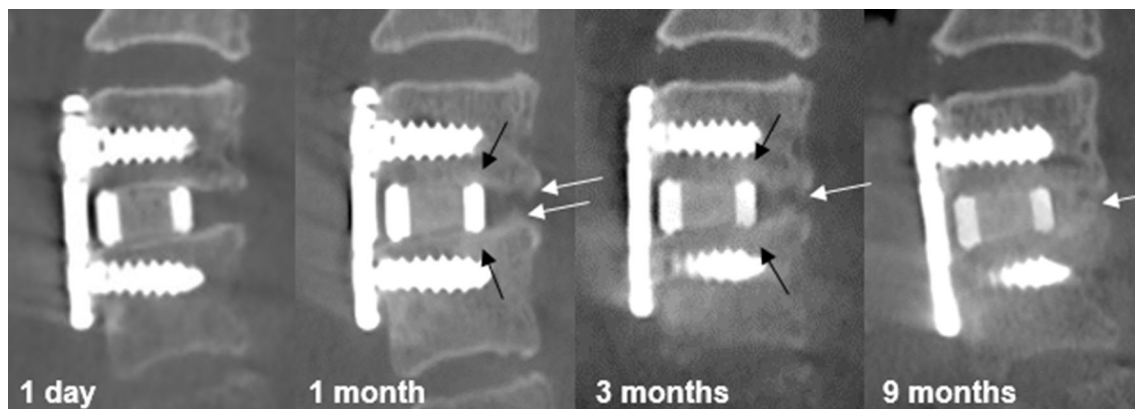
Regarding bone formation within the disc space posteriorly to the cage, firstly radiodense thickening of the endplates is seen in the form of stalactites and stalagmites (at 1 month), followed by gradually filling in of the disc space with hazy densities representing matrix mineralization (progressively at 3 and 6 months). Finally, at 9 months, CBCT images show an almost solid trabecular

bone bridge. While at a single sagittal image, this bone bridge extending from the vertebra below to the vertebra above may seem a thin pillar, the axial CBCT images demonstrate that the bony fusion consists of left-to-right broad struts.

Another qualitative finding consists of the bone changes at the interface between the cages and the endplates. Already after 1 month, dense sclerotic bone change is seen underlying the endplates at the pressure areas with the cage wall. These pressure areas in this case are at the posterior half of the cage. On the sagittal image, the sclerotic bone change has the shape of the hood of a mushroom on top of its stalk (the cage wall). This sclerotic bone change becomes only slightly wider in shape at the different time points. Subsidence of the cage into the vertebral body is not seen.
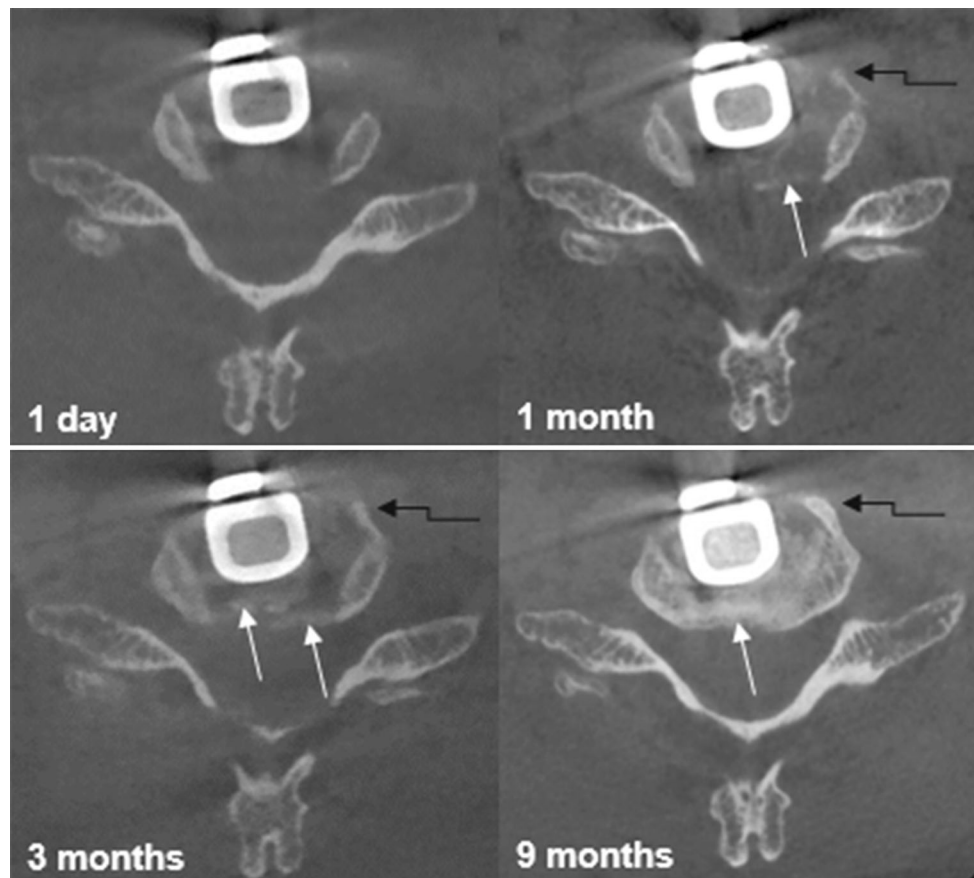
A third qualitative finding relates to the changes at the interface between the bone graft filler and the endplates. One day after surgery, a clear radiolucent line is seen in between, which gradually changes into a radiodense area representing bony integration of the bone graft filler with the vertebral body. Bony integration is first seen with the vertebra above (at 1 month) and later with the vertebra below (at 9 months). Note that metal artefacts were present as broad, slightly radiodense bands running obliquely through the image on both sides of the anterior plating.

Axial CBCT images demonstrate the ability of CBCT to evaluate the radiodensity of the bone graft filler within the circumferentially radiodense cage, not possible on radiographs. The density of the bone graft filler inside the cage gradually increases over the different time points (Fig. 3). We also observed the appearance of hazy densities

Fig. 2 Sagittal CBCT images of 1 day, 1, 3 and 9 months post-operatively provide qualitative assessment of bony changes at the interface between cage wall and vertebral endplates, in the intervertebral disc space, and between bone graft filler and vertebral endplates. Dense sclerotic bone apposition underlying the endplates is seen at the interface between the posterior cage wall and vertebral endplates, resembling the hood of a mushroom on its stalk (cage wall): reactive bone changes at pressure points (*black arrows*). In the disc space posteriorly, bony apposition to the endplates in the form of stalactites and stalagmites is seen together with hazy densities in the centre (matrix mineralization), resulting in solid trabecular bone fusion at 9 months (*white arrows*). The radiolucent line between bone graft filler and the endplates fills in with radiodense material (above at 1 month and below at 9 months), representing osseointegration of the bone graft filler with the endplates

Fig. 3 Axial views at 1 day, 1, 3 and 9 months post-operatively enable quantitative assessment of bone graft filler density and of bone formation in the disc space around the cage. CBCT allows the measurement of radiodensity changes of the bone graft filler within a circumferentially radiodense cage, not possible with radiography or classic CT scan. Note that the density of the bone graft filler inside the cage gradually increases over the different time points. The CBCT images at 1 and 3 months show hazy densities in the disc space posteriorly to the cage, representing bone mineralization, followed by a solid trabecular bone bridge at 9 months (*white arrows*). Another strut of bone fusion can be seen developing on the left anterolateral side of the disc space (*black arrow*). CBCT allows for appreciation of the width and size of the bone formation within the disc space around (posteriorly and laterally of) the cage. Note the width of the hazy densities (bone mineralization) posteriorly to the cage, a width that cannot be seen with either radiography or classic CT scan

posteriorly of the cage 1 month after the surgery, which increased in amount and density 3 months post-operatively, and have changed into trabecular bone at 9 months post-operatively.

Discussion

CBCT provides high-resolution cross-sectional imaging of the cervical vertebrae in the presence of metal implants while maintaining a low-radiation dose. In this case report, CBCT was successfully used to evaluate the process of bony fusion after ACIF. For the first time, in vivo imaging evaluation of the bone graft filler within the centre of a circumferentially radiodense hydroxyapatite cage was achieved, both quantitatively and qualitatively. Quantitative density measurements using greyscale units showed a steady increase in bone graft filler density over the course of 9 months. Greyscale analysis of CBCT images had a very high agreement between the independent investigators. Qualitatively, bony integration of the bone graft filler with the adjacent vertebrae was shown as disappearance of the radiolucent line in between. Both these findings have yet not been possible neither with radiographic nor classical CT imaging.

Of note, while the greyscale values of the images provided by CBCT do not allow the direct determination of HU, the accepted standard for measuring radiodensity and thus matrix calcification in the process of bone formation, recent work by Razi et al. [9] has demonstrated a linear relationship between CBCT greyscale and HU. Their work was done using the same type of CBCT that we used (NewTom 5G CBCT) and thus supports the feasibility of our method in assessing density changes [9].

The high-resolution cross-sectional technique of CBCT offers a detailed qualitative evaluation of the bone fusion process. Besides the subchondral sclerotic bone changes at the pressure areas of the cage wall with the endplates, different stages of the bone fusion process were shown in the periphery of the cage: bone apposition adjacent to the endplates, appearance of hazy densities indicating matrix calcification/mineralization, and finally formation of trabecular bone within the disc space. Appreciation of the amount and width of these changes was possible with this cross-sectional technique, not demonstrated before with radiography nor with classical CT. With regard to predicting ACIF outcomes, CBCT may demonstrate the amount of bone mineralization is visible, as there are the hazy densities visible before a stable bone bridge is formed [10, 11].

In comparison to conventional CT imaging, CBCT delivers a comparable or lower radiation dose to the patient. In a comparison between effective radiation dose of CBCT and Multislice CT (MSCT) scanners for dental and maxillofacial applications, effective dose values ranged from 13 to 82 μSv for CBCT and from 474 to 1160 μSv for MSCT [5]. Similar data concerning a significant decrease in radiation dose values have been reported elsewhere [4, 6]. Considering the number of scans or radiographic examinations obtained in a typical ACIF procedure, from initial diagnosis through the end of treatment, it seems prudent then to limit the patient's exposure and therefore obviate the potentially deleterious effects of radiation exposure.

Another advantage of CBCT is that metal artefacts do not influence CBCT image quality as much as they do with classical CT [12, 13]. Most ACIF procedures will use some manner of metal implant, either stainless steel or titanium, in the procedure. Admittedly, CBCT does suffer from artefact immediately next to the anterior plate [14, 15]. This does not, however, extend to the entire volume involved in the fusion procedure, and the artefact diminishes rapidly with distance from the implant [15]. Therefore, while a small percentage of the imaged volume will be affected by implant artefact, CBCT still provides good imaging quality through the overwhelming majority of the imaged volume. In our case, metal artefacts of the anterior plate were seen as slightly radiodense bands running obliquely through the image. These artefacts did not prohibit the qualitative evaluation of bony changes at the ACIF level. Quantitative information was expected to be influenced by these metal artefacts, but we tried to minimize this influence by positioning the patient identically at each time point resulting in a comparable metal artefact for each scan.

As an imaging technique, CBCT offers some clear advantages over CT or radiographs. As with any tool and original applications, it is necessary to develop the full potential in this specific function. Further research is warranted to determine the best way to analyse CBCT images. It would be helpful to expand on the initial work by Razi et al. [9] and further elucidate the relationship between HU and CBCT greyscale measure, as well as the relationships between the greyscale units and fusion, bony ingrowth and trabecular bridging. Further studies should examine the variability of changes as observed in imaging during the process of bone fusion using a large patient cohort. While our study presents the first use of CBCT to assess bone fusion following ACIF, this pilot work supports the clinical application to analyse bone fusion process in detail and also supports the potential to study in vivo the osseointegration of the bone graft filler within the cage.

Compliance with ethical standards

References

1. Miracle AC, Mukherji SK (2009) Conebeam CT of the head and neck, part 2: clinical applications. AJNR Am J Neuroradiol 30:1285–1292
2. Casselman JW, Quirynen M, Lemahieu SF, Baert AL, Bonte J (1988) Computed tomography in the determination of anatomical landmarks in the perspective of endosseous oral implant installation. J Head Neck Pathol 7:255–264
3. Jacobs R (2011) Dental cone beam CT and its justified use in oral health care. JBR-BTR 94:254–265
4. Pauwels R, Beinsberger J, Collaert B, Theodorakou C, Rogers J, Walker A, Cockmartin L, Bosmans H, Jacobs R, Bogaerts R, Horner K, Consortium SP (2012) Effective dose range for dental cone beam computed tomography scanners. Eur J Radiol 81:267–271
5. Loubele M, Bogaerts R, Van Dijck E, Pauwels R, Vanheusden S, Suetens P, Marchal G, Sanderink G, Jacobs R (2009) Comparison between effective radiation dose of CBCT and MSCT scanners for dentomaxillofacial applications. Eur J Radiol 71:461–468
6. Ludlow JB, Ivanovic M (2008) Comparative dosimetry of dental CBCT devices and 64-slice CT for oral and maxillofacial radiology. Oral Surg Oral Med Oral Pathol Oral Radiol Endod 106:106–114
7. Ruivo J, Mermuys K, Bacher K, Kuhweide R, Offeciers E, Casselman JW (2009) Cone beam computed tomography, a low-

dose imaging technique in the postoperative assessment of cochlear implantation. Otol Neurotol 30:299–303

8. De Vos W, Casselman J, Swennen GR (2009) Cone-beam computerized tomography (CBCT) imaging of the oral and maxillofacial region: a systematic review of the literature. Int J Oral Maxillofac Surg 38:609–625

9. Razi T, Niknami M, Alavi Ghazani F (2014) Relationship between Hounsfield Unit in CT Scan and Gray Scale in CBCT. J Dent Res Dent Clin Dent Prospects 8:107–110

10. Morgan EF, Mason ZD, Chien KB, Pfeiffer AJ, Barnes GL, Einhorn TA, Gerstenfeld LC (2009) Micro-computed tomography assessment of fracture healing: relationships among callus structure, composition, and mechanical function. Bone 44:335–344

11. McKinley DW, Chambliss ML (2000) Follow-up radiographs to detect callus formation after fractures. Arch Fam Med 9:373–374

12. Kovacs M, Fejerdy P, Dobo NC (2008) Metal artefact on head and neck cone-beam CT images. Fogorv Sz 101:171–178

13. Bechara BB, Moore WS, McMahan CA, Noujeim M (2012) Metal artefact reduction with cone beam CT: an in vitro study. Dentomaxillofac Radiol 41:248–253

14. Schulze RK, Berndt D, d'Hoedt B (2010) On cone-beam computed tomography artifacts induced by titanium implants. Clin Oral Implant Res 21:100–107

15. Benic GI, Sancho-Puchades M, Jung RE, Deyhle H, Hammerle CH (2013) In vitro assessment of artifacts induced by titanium dental implants in cone beam computed tomography. Clin Oral Implant Res 24:378–383